Characterization of Gold(I) in Dealuminated H-Mordenite Zeolite

Mohamed M. Mohamed,*,† Tarek M. Salama,‡ Ryuichiro Ohnishi,§ and Masaru Ichikawa§

Benha University, Faculty of Science, Department of Chemistry, Benha, Egypt, Al-Azhar University, Faculty of Science, Department of Chemistry, Naser City 11884, Cairo, Egypt, and Catalysis Research Center, Hokkaido University, Sapporo 060, Japan

Received October 4, 2000. In Final Form: March 7, 2001

The CO interaction with Au^+/dealuminated H-mordenite as well as with the nondealuminated samples, at room temperature, after evacuation at different temperatures (343, 393, 453, and 573 K) has been studied by in situ Fourier transform infrared spectroscopy. The Au^+−CO band at 2192 cm^{-1} of the dealuminated sample showed a remarkable thermal stability on raising the temperature (till 473 K) for the degassed sample at 393 K, compared with the nondealuminated one. It has been revealed from the X-ray diffraction and X-ray photoelectron spectroscopy (XPS) analyses that the nonframework Al species were formed and embedded inside the zeolite lattice. The latter species were found to be responsible for the stability of CO coordinated Au^+. The XPS data also showed the easier reduction of Au^{n+} species in the nondealuminated sample compared with the dealuminated one, as revealed from the peak area ratio Cl 2p/Au 4f. Adsorption of CO onto Au^+/dealuminated H-mordenite, after evacuation at 343 K, produced a broad band at 1949 cm^{-1} attributed to bridged bonded CO species. This was confirmed by the relative increase in intensity of this band (Au−CO−Au) compared with the linearly bonded one at 2192 cm^{-1} during thermal evacuation till 473 K. The temperature-programmed reduction profile of Au^{n+}/dealuminated H-mordenite samples revealed, in concordance with the IR and XPS data, the better stability of the Au^+ state in dealuminated samples as compared with nondealuminated ones.

Introduction

Gold has attracted little attention in the area of heterogeneous catalysis because of its inertness compared with platinum group catalysts.[1−3] However, it has recently been emphasized that well-dispersed Au^+ species inside NaY and ZSM-5 zeolites exhibited high activity for chemisorption of NO and CO and also in NO + CO and direct NO decomposition reactions.[4−6] In addition, a dual site of Au^+ and Au^0 was responsible for activating the CO + H_2O (WGS) reaction at low temperature (323 K) when incorporated inside zeolites such as NaY, Na-ZSM-5, and Na-mordenite.[7,8] It was acknowledged that gold agglomerates as big metallic particles during catalyst preparation at temperatures close to 373 K because of its low sublimation energy, indicating instability of gold.[9] Therefore, it is important to improve the thermal stability of the charged Au^{n+} moieties, in particular the Au^+ state that acts as an active site for the above-mentioned reactions.

In view of the importance of coordinatively unsaturated (cus) Al ions for supporting different metal cations such as Co, Mg, and Cr,[10] the mild steam dealumination of H-mordenite was undertaken for the purpose of generating Al cus sites that could act as anchoring sites for the charged Au^ICl species. The importance of acid sites in zeolites as a consequence of dealumination evoked us to study the nature of gold species encapsulated inside the dealuminated H-mordenite zeolite. It has been reported that Au^+ incorporated inside zeolite channels interacted with CO to form carbonyls. However, the reversibility of CO adsorption on Au(I) at about 323 K underlined the activities of Au^+ species toward any catalytic reaction involving CO.[4,5] From the intriguing properties of Au^{n+}/zeolite catalysts and the morphological changes at relatively low temperatures, which affect the catalytic performances of gold in some reactions,[4−9] much care should be taken to eliminate such an instability problem of Au(I) in carbonylation. To the best of our knowledge, the resistance to temperature change of adsorbed CO to Au^+/zeolite has not been reported in the literature until now.

Therefore, the objective of the current study is to stabilize the Au^+ site through incorporation inside the dealuminated H-mordenite zeolite. This study was further undertaken to examine, for the first time, the possibility of forming bridged bonded carbonyl species under the humid condition obtained after dealumination.

Experimental Section

1. Catalyst Preparation. The steam dealuminated H-mordenite (dM) sample was carried out under mild steaming conditions at 773 K and $P_{H_2O} = 1.00 \times 10^4$ Pa for 45 min. The dealuminated H-mordenite sample was prepared with am-

* To whom correspondence should be addressed. Tel: 2013-222-578. Fax: 2013-222-578. E-mail: mohmok2000@yahoo.com.
† Department of Chemistry, Benha University.
‡ Department of Chemistry, Al-Azhar University.
§ Catalysis Research Center, Hokkaido University.

(1) Haruta, M.; Yamada, W.; Kobayashi, T.; Ligima, S. *J. Catal.* **1989**, *115*, 301.
(2) Bond, G. C.; Sermon, P. A. *Gold Bull.* **1973**, *6*, 102.
(3) Galvano, S.; Parravano, G. *J. Catal.* **1987**, *55*, 178.
(4) Qiu, S.; Ohnishi, R.; Ichikawa, M. *J. Chem. Soc., Chem. Commun.* **1992**, 1425.
(5) Salama, T. M.; Qiu, S.; Ohnishi, R.; Ichikawa, M. *Shokubai* **1994**, *36*, 86.
(6) Salama, T. M.; Shido, T.; Ohnishi, R.; Ichikawa, M. *J. Chem. Soc., Chem. Commun.* **1994**, 2749.
(7) Mohamed, M. M.; Salama, T. M.; Ichikawa, M. *J. Colloid Interface Sci.* **2000**, *224*, 366.
(8) Mohamed, M. M.; Ichikawa, M. *J. Colloid Interface Sci.* **2000**, *232*, 381.
(9) Haruta, M.; Kobayashi, T.; Sano, H.; Yamada, N. *Chem. Lett.* **1987**, 405.
(10) Richter, M.; Parlitz, B.; Eckelt, R.; Frike, R. *J. Chem. Soc., Chem. Commun.* **1997**, 383.

10.1021/la001403f CCC: $20.00
Published on Web 08/04/2001

monium hexafluorosilicate (AHF) using the method of Skeels and Breck.[11] The 5 wt % Au dealuminated (Au/dM) and nondealuminated H-mordenite (Au/ndM) samples were prepared at room temperature by mechanical mixing of $AuCl_3 \cdot 2H_2O$ (Strem Chemicals, 99% purity) with dM and ndM zeolites under a nitrogen atmosphere. The samples were evacuated in a conventional high vacuum (10^{-6} Torr) manifold while slowly ramping the temperature (0.2 K min^{-1}) up to 338 K, where the exchange reaction was conducted for 48 h. The $AuCl_3$ crystallites vaporized upon heating and diffused inside the zeolite channels where the following reaction occurred: $AuCl_3 + 2H_2O\text{-}Z \rightarrow AuCl/Z + 2\ HCl + 2\ OH/Z$, where Z refers to zeolite in general. The evolution of gaseous HCl is monitored by the temperature programmed desorption (TPD) technique, as an indication of the interaction of $AuCl_3$ with H_2O contained in the zeolite sample.[12]

2. In Situ Fourier Transform Infrared (FT-IR) Spectroscopy. In situ FT-IR spectra of 50 Torr CO (1 Torr = 133.3 N m^{-1}) adsorption were carried out in a closed circulation system with a dead volume of 189 cm^3. An IR cell equipped with NaCl windows was used for treatment and measurements. A self-supported wafer (20 mg) was prepared under a nitrogen atmosphere and mounted to the sample holder in the IR cell. The wafer was evacuated at the desired temperature for 30 min before adsorption at room temperature. The IR spectra were recorded with a resolution of 2 cm^{-1} using a Shimadzu double beam FT-IR 4100 spectrometer. The spectra for the support background during the CO chemisorption were subtracted from the sample spectra.

3. Inductively Coupled Plasma Atomic Emission (ICP) Spectrosopy. The dealuminated and nondealuminated samples were analyzed for Si and Al using ICP spectroscopy (Perkin-Elmer, Optima 3000).

4. X-ray Diffraction (XRD). The X-ray patterns for the samples were collected on an MXP-3 (Mac Science Co., Ltd.) automated powder diffractometer by using Ni-filtered Cu Kα radiation.

5. X-ray Photoelectron Spectroscopy (XPS). The XPS analysis was achieved using a Kratos XSAM 8000 PCI instrument. Al Kα (1486.6 eV) radiation from a Mg/Al dual anode X-ray source (10 kV, 20 mV) was used. The base pressure in the analysis chamber was well below 1×10^{-9} Torr during the measurements.

6. Temperature-Programmed Reduction (TPR). TPR experiments were performed using an automated gas adsorption analyzer (Altamira AMI-1). The catalyst (50 mg) was loaded in a quartz microreactor and heated from 298 to 323 K (heating rate 5 K min^{-1}) in a flow of helium (20 mL min^{-1}). The sample was then subjected to a H_2/argon flow mixture (15 mL min^{-1}, 9.98% H_2 in argon) to obtain the H_2 consumption values, which was performed using a dry ice/acetone trap to prevent any water interference peaks. The temperature was linearly increased from 323 to 773 K at a ramping rate of 5 K min^{-1}.

Results and Discussion

1. XRD Analysis. The X-ray diffraction patterns of the parent H-mordenite, dM, Au/dM, and Au/ndM samples are shown in Figure 1. The steam dealuminated H-mordenite zeolite exhibited the same crystalline pattern of the parent H-mordenite sample. It appears that the crystal structure of the steam dealuminated sample is not collapsed or even distorted under the treatment conditions used. No lines due to the $AuCl_3$ crystalline phase (2θ = 12.9°, 14.7°, 22.0° for Cu Kα) appeared after heat treatment at 338 K for Au/dM and Au/ndM samples. This implies that $AuCl_3$ is highly dispersed and probably is located in the internal surface of the zeolite, similar to what has been reported formerly on $AuCl_3$/NaY[13] and CuCl/NaY.[14] From the XRD patterns, the Au metallic

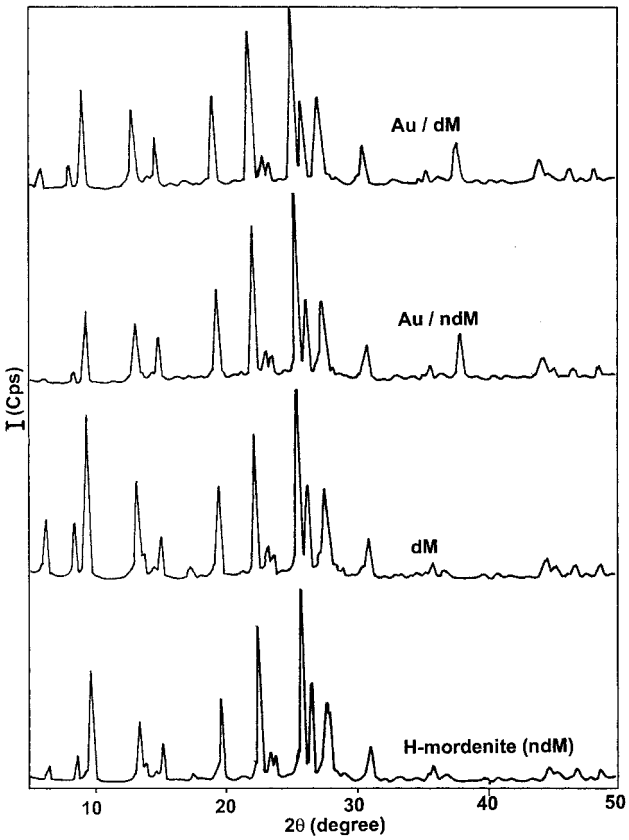

Figure 1. Powder X-ray diffraction patterns of H-mordenite (ndM), steam dealuminated H-mordenite (dM), Au/ndM-338 K, and Au/dM-338 K.

phase at 2θ = 38.15° and 44.40° was observed for Au/dM and Au/ndM samples. They were the characteristic diffraction lines of Au(111) and Au(200), respectively. This suggested the reduction of $AuCl_3$ into lower oxidation states upon migration and interaction with H_2O molecules in zeolite channels at 338 K.[12,15] This undoubtedly indicated that reduction occurred inside the zeolite channels. The same conclusion has been obtained for NaY zeolite.[12] The reduction process was emphasized by noting that the red color of $AuCl_3$ turned to the pale yellow color of AuCl. The mean crystallite diameters of gold metal (determined by the Scherrer equation) were found to be 55 and 70 Å for Au/dM and Au/ndM, respectively. This suggested that there is a strong interaction between gold species and dM zeolite that has the effect of hindering the Au sintering. The above result was further emphasized by examining the *d*-values of some diffraction lines such as 2.86, 3.26, 5.88, 9.36, and 10.27 of zeolite in Au^{n+}/dM and Au^{n+}/ndM samples. Similarly, it has been reported by Haruta et al.[16] that a decrease in Au particle size when supported on transition metal oxides, such as α-Fe_2O_3, Co_3O_4, and NiO, was obtained and attributed to the strongly held Au by the support oxides.

The XRD unit cell parameters of dealuminated and nondealuminated H-mordenite and Au catalysts encapsulated in them are summarized in Table 1. These parameters were deduced in a similar way to that of

(11) Skeels, G. W.; Breck, D. W. *Proceedings 6th International Zeolite Conference*; Olson, D., Bisio, A., Eds.; Batterworths: GuildFord, 1984; p 87.

(12) Salama, T. M.; Shido, T.; Minagawa, H.; Ichikawa, M. *J. Catal.* **1995**, *152*, 322.

(13) Qiu, S.; Ohnishi, R.; Ichikawa, M. *J. Phys. Chem.* **1994**, *98* (11), 2719.

(14) Xie, Y. C.; Tang, Y. Q. *Adv. Catal.* **1990**, *37*, 187.

(15) Salama, T. M.; Shido, T.; Ohnishi, R.; Ichikawa, M. *J. Phys. Chem.* **1996**, *100*, 3688.

(16) Haruta, M.; Yamada, N.; Kobayashi, T.; Iijima, S. *J. Catal.* **1989**, *115*, 301.

Table 1. XRD Unit Cell Parameters of Dealuminated (dM) and Nondealuminated (ndM) H-Mordenite Encapsulated Gold Catalysts[a]

sample and treatment	*a* (Å)	*b* (Å)	*c* (Å)	*V* (Å)^3	crystallinity %	Al_t	Al_f	Al_{nonf}
H-mordenite (parent)	19.229	20.356	7.493	2932.95	100	6.5 (6.4)	6.5	
Au/H-mord (Au/ndM)	18.240	20.234	7.486	2762.84	63			
steam deal (dM)	18.184	20.400	7.486	2776.95	101	6.5 (10.2)	4.3	2.2
Au/steam deal (Au/dM)	18.200	20.404	7.489	2781.06	75			
F/deal (dMf)	18.201	20.381	7.493	2779.72	114	6.5 (12.3)	3.6	2.9
Au/deal-F (Au/dMf)	18.220	20.383	7.496	2783.85	90			

[a] The crystallinity was obtained from the sum of the intensities of the 111, 130, 241, 002, 511, and 530 diffraction lines. The original H-mordenite was taken as a reference of 100% crystallinity. *V* is the unit cell volume *abc*. Al_t is the absolute Al total content determined by ICP. Al_f is the number of framework Al per unit cell (uc). Values in parentheses are Si/Al ratios. Al per unit cell of the parent sample was obtained from the following equation (ref 17): Al/uc = 48/[(Si/Al) + 1]. Al_{nonf} is the fraction of Al in a nonframework position.

Meyers et al.,[18] who studied aluminum deficient mordenites by different methods. The length of the *c* axis did not vary significantly between catalyst samples, though the most significant changes were in the direction of the *a* axis. However, after AHF treatment a decrease in the *a* value was attained whereas the *b* value showed an expansion. The obtained contraction after steaming is attributed to the expulsion of some aluminum atoms from the framework into extraframework positions. This result was in agreement with the finding of Makarova et al.[19] On the other hand, an expansion following Au incorporation for some unit cell dimensions was noted. A formula[17] for estimating the framework aluminum and consequently the nonframework Al species can easily be deduced through the values of Si/Al ratios determined by ICP.[20] The dislodged Al atoms and their influences on stabilization of different Au species compared with the local Al environment are given below.

The sum of the intensities of 111, 130, 241, 002, 511, and 530 diffraction lines was used to calculate the degree of crystallinity of the samples with respect to the H-mordenite, which was taken as a reference (100%). As indicated in Table 1, the crystallinity of the dealuminated samples was similar to that of the parent sample. The crystallinity decreased after Au insertion, however, and the Au^{n+}/ndM sample was particularly more susceptible to the crystallinity loss compared with the Au^{n+}/dM sample.

2. XPS Analysis. The XPS binding energy values of the revelant element of the parent, Au^{n+}/dM and Au^{n+}/ndM, evacuated at 393 K, are presented in Table 2. The binding energy (BE) values were corrected with the Si (2p = 104.40 eV) peak of H-mordenite zeolite, which was taken as a reference. The Au species supported on the dM zeolite showed higher BE values compared with those on the ndM ones. The XPS Au 4f binding energies of Au^{3+}, Au^+, and Au^0 obtained from Au^{n+}/dM catalysts were 89.30, 86.10, and 85.30 eV, respectively. These values were higher by 0.25, 0.25, and 0.13 eV than the corresponding values for the Au^{n+}/ndM sample, respectively. This reflects the higher stability of the Au species in the dealuminated sample than in the nondealuminated one. As a further confirmation, the manifested atomic concentrations for different Au states in the Au^{n+}/ndM sample were higher by a factor of approximately 2.0 compared with those for the Au^{n+}/dM sample. This undoubtedly proved that Au species were more accessible to the intra-zeolite lattice in the dM sample, whereas it was located near the surface in the ndM sample. A decrease in the concentration of Al 2p in the Au^{n+}/dM sample compared with the Au^{n+}/ndM was also noticed. This could be due to the dislodgment of some Al species, as a result of steaming, inside the mordenite channels in the former sample. This could be correlated with the decreased Au species concentrations on the surface for this sample to highlight the easier interaction of Au species with the nonframework Al inside the dM lattice.

Table 2. XPS Results of Au^{n+} Entrapped in Dealuminated (dM) and Nondealuminated (ndM) H-Mordenite Zeolite

sample	element	binding energy/eV	atomic concn %
Au^{n+}/dM	Si 2p	104.40	52.37
	Al 2p	75.40	5.33
	O 1s	534.50	41.03
	Au^0 4f	85.30	0.40
	Au^+ 4f	86.10	0.34
	Au^{3+} 4f	89.30	0.50
	Cl 2p	200.00	0.03
Au^{n+}/ndM	Si 2p	104.40	47.81
	Al 2p	75.55	8.20
	O 1s	534.15	41.74
	Au^0 4f	85.17	0.70
	Au^+ 4f	85.85	0.54
	Au^{3+} 4f	89.05	0.99
	Cl 2p	200.00	0.02

The increase in the O 1s BE value by 0.35 eV in the Au^{n+}/dM sample compared with that in Au^{n+}/ndM indicates a decrease in the electron density of oxygen atoms in the former sample. To describe the electronic feature of Au^{n+}/dM, a bonding model is proposed. It is expected on the basis of the electronic feature of zeolite that the basic strength of lattice oxygen in zeolite is enhanced as the charges of metal ions decrease.[21] Accordingly, the stability of the Au species of a lower charge (i.e., Au^+) on dM in comparison with that of the higher charge (i.e., Au^{3+}) is anticipated.

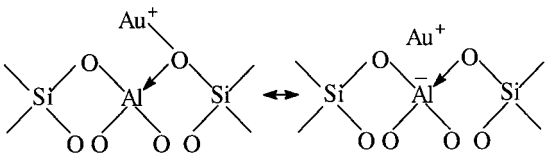

On the other hand, the observed Cl 2p BE at 200.0 eV for both Au/dM and Au/ndM catalysts was much higher than that for the terminal Cl atoms in $KAuCl_4$ (198.10 eV), indicating that the bridged Au−Cl−Au structure prevails because a less negative charge on the bridged Cl

(17) Ribotta, A.; Miro, E.; Lombardo, E.; Petunchi, G.; Moreaux, C.; Dereppe, G. M. *J. Catal.* **1997**, *168*, 511.
(18) Meyers, B. L.; Fleisch, T. H.; Ray, G. J.; Miller, J. T.; Hall, J. B. *J. Catal.* **1988**, *110*, 82.
(19) Makarova, M. A.; Garforth, A.; Zholobenko, V. L.; Dwyer, J.; Earl, G. J.; Rawlenence, D. *Studies in Surface Science and Catalysis*; Weitkamp, J., Karge, H. G., Pfeifer, H., Holderich, W., Eds.; Elsevier: Amsterdam, 1994; Vol. 84.
(20) Sohn, J. R.; De Canio, S. J.; Lunsford, J. H.; Donnell, D. J. O. *Zeolites* **1986**, *6*, 225.
(21) Okamoto, Y.; Ogawa, M.; Maezawa, A.; Imanaka, T. *J. Catal.* **1988**, *112*, 427.

atoms is expected.[22] This indicates undoubtedly the involvement of terminal Cl atoms rather than bridged Cl atoms during the reduction process. It was shown that the structure of AuCl is polymeric with zigzag chains of Au and Cl atoms, with each Cl bridging between Au atoms.[23,24] The Cl 2p intensity ratios were found to be less than those expected. This may be due to the fact that Cl has low surface sensitivity. Furthermore, the expected interaction between $AuCl_n$ species and the residual water in zeolite, resulting in free Cl atoms desorbed as HCl,[12] could be another plausible explanation. The desorption of Cl_2 was not evident, but a large amount of HCl ($m/e = 36$) was found to desorb in a TPD-mass study of the interaction of H_2O contained in NaY zeolite and $AuCl_3$ species.[12] The evolution of HCl is obtained because of the hydrolysis of $AuCl_3$ by H_2O. By use of the peak areas of Au 4f and Cl 2p and the relevant elemental sensitivity factor (4.95 for Au 4f and 0.73 for Cl 2p),[25,26] the $(Cl/Au)_{surface}$ values were 0.5 for Au^{n+}/dM and 0.16 for Au^{n+}/ndM. This gives a clue that the reduction process of Au^{n+} proceeded more readily in ndM than in dM. In other words, charged Au species are more stable in the dM sample than in ndM.

3. In Situ FT-IR of CO Adsorption as a Function of Treatment Temperatures. Figure 2 shows the IR spectra of CO adsorption on the Au^{n+}/dM sample pretreated in a vacuum (10^{-5} Torr) at 343, 393, 453, and 573 K, before the admission of gas at room temperature. Following this, the sample was degassed at the same pretreatment temperatures. An intense and sharp IR band at 2192 cm^{-1} appears in spectrum a in Figure 2 with a minor band at 2128 cm^{-1}. Besides, a shoulder at 2180 cm^{-1} was also observed. The band at 2192 cm^{-1} is ascribed to CO chemisorbed on Au^+ sites, whereas the 2128 cm^{-1} band is attributed to CO adsorbed on Au metal.[15] The assignment of the former band comes from a band shift to frequencies higher than that of free CO at 2155 cm^{-1}.[15] The high-frequency shift of the Au^+-CO (ca. 16 cm^{-1}) species relative to that previously reported for $CO \rightarrow Au^+/W$ (2176 cm^{-1}) is interpreted in terms of CO attached on Au^+ species with acidic Al^{3+} and H^+ sites in the zeolite channels.[26] It can be seen that an increase in intensity for the band at 2180 cm^{-1} during evacuation at 393 K (spectrum b), that has been shown as a shoulder in spectrum a, was revealed. The persistence of the 2180 cm^{-1} band at this temperature indicates that it is derived from CO interacting with Au^+ that could be located near the surface. The presence of different types of CO species on the surface, for example, CO on Au^{n+} with slightly variable n ($0 \leq n \leq 1$), could be responsible for the maximum band shift from 2192 to 2180 cm^{-1}. Consequently, the 2192 cm^{-1} band is most likely assigned to CO binding to intra-zeolite Au^+ species. Upon increasing the evacuation temperature of the sample to 453 K (spectrum c), a marked decrease in intensity of the Au^+-CO/dM band at 2180 cm^{-1} is obtained. The dominance of the 2192 cm^{-1} band at 453 K at the expense of the 2180 cm^{-1} band indicates the stability of the species derived from the former band. By increasing the evacuation temperature to 573 K, the intensity of the Au^+-CO band is greatly diminished (spectrum d).

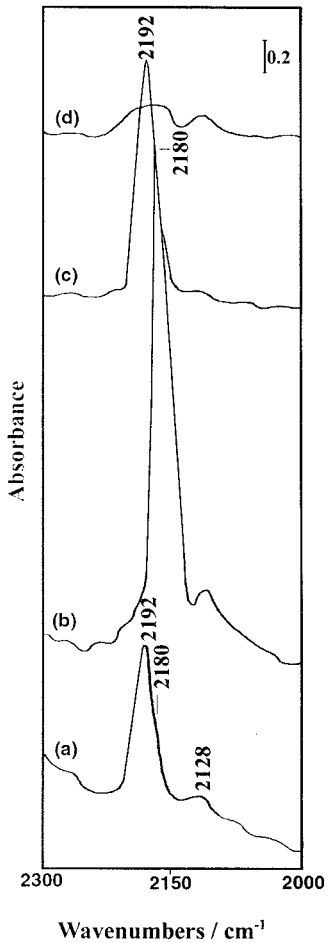

Figure 2. In situ FT-IR spectra of CO (50 Torr, exposure time 5 min) adsorbed at room temperature on the Au^+/dM sample pretreated in a vacuum (10^{-5} Torr) at (a) 343, (b) 393, (c) 453, and (d) 573 K. The system was evacuated at the same pretreatment temperatures for 15 min.

Figure 3 shows the IR spectra of CO adsorption at room temperature on the Au^+/dM sample previously evacuated at 393 K for $^1/_2$ h. The monotonic increase of evacuation temperature of CO showed major stability for the 2180 cm^{-1} band up to 473 K and a measurable intensity up to 508 K. The 2180 cm^{-1} band, which is preserved to support its dependence on the stability of the Au^+-CO moiety, demonstrates the substantial presence of Au^+ sites relative to a small fraction of Au^0. This band was shifted to 2188 cm^{-1} at 508 K as a result of diminishing CO population. The integrated peak area of 2180 cm^{-1} is 18 times larger than that of 2128 cm^{-1} at 473 K. We can conclude that CO adsorption on the surface is very high to nearly 100% of the total Au content, assuming homogeneous distribution of Au species. This unusual stability of Au^+-CO species inside dM can be explained in the view of the strong σ bond formed between the coordinatively unsaturated cation and CO, as has been already noted for the Cu^+-CO/ZSM-5 catalyst.[27] Interestingly, the Au^+-CO bond is more strengthened because of the presence of the unsaturated coordinated Al species in the dealuminated sample. The presence of Au^+ species minimizes the back π bonding, from the d electrons of the metal cations to the π^* antibonding orbitals of the CO molecules leading only to

(22) Koley, P. A.; Nirmala, R.; Prasad, L. S.; Ghosh, S.; Manoharan, P. T. *Inorg. Chem.* **1992**, *31*, 1764.
(23) Janssen, E. M. W.; Folmer, J. C. W.; Wieger, G. A. *J. Less-Common Met.* **1974**, *38*, 71.
(24) Straehle, J.; Loercher, K. P. *Z. Naturforsch.* **1974**, *B29*, 266.
(25) Briggs, D.; Seah, M. P. In *Practical Surface Analysis, Auger and X-ray Photoelectron Spectroscopy*; John Wiley & Sons: New York, 1990; Vol. 1.
(26) Huber, H.; McIntosh, D.; Ozin, G. A. *Inorg. Chem.* **1977**, *16*, 976.
(27) Maache, M.; Janin, A.; Lavalley, J. C.; Benazzi, E. *Zeolites* **1995**, *15*, 507.

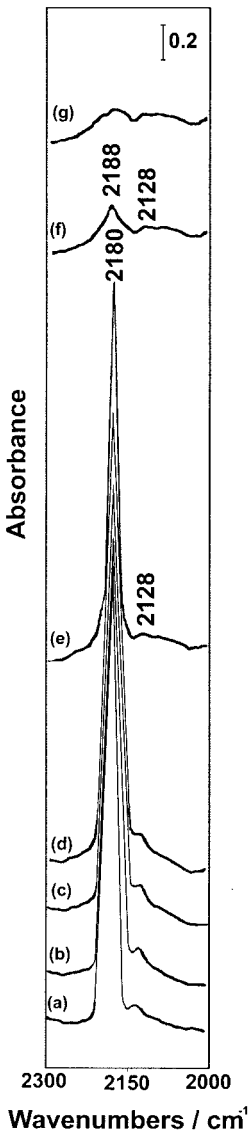

Figure 3. In situ FT-IR spectra of CO (50 Torr) adsorbed at room temperature on the Au^+/dM sample, after treatment at 393 K for $^1/_2$ h. The system was evacuated while raising the temperature to (a) 308, (b) 323, (c) 373, (d) 423, (e) 473, (f) 508, and (g) 521 K

a strong σ bond that plays the determining role for the properties of the carbonyls rather than π bonding.[27,28]

Further insight into the stability of the 2180−2188 cm^{-1} band after different evacuation temperatures is shown in Table 3. The quantitative regard of CO chemisorption at room temperature onto Au^+/dM and Au^+/ndM samples has been calculated from the absorptivities of Au^+−CO sites using the Lambert−Beer law. This was possible because of the knowledge of the molar extinction coefficient of the CO molecules in the 2140−2200 cm^{-1} range that is equal to 2.7 cm μmol^{-1}.[28] It was found that the numbers of Au^+ ions accessible to CO in the dM samples were greater than on the ndM ones. The high stability observed for the Au^+→CO inside the dM sample compared with the ndM one is interpreted in terms of the existence of cus Al sites induced by dealumination. These sites were validated through XRD analysis that showed the possible formation of the nonframework Al species with steaming as well as

Table 3. Quantitative Results of Au^+ Ions Accessible to CO Adsorption as a Function of Increasing the Evacuation Temperatures

	Au^{n+}/dM		Au^{n+}/ndM	
pretreatment temp (K)	A^a	CO−Au^+ [b] (μmol/cm^2)	A	CO−Au^+ (μmol/cm^2)
343	0.26	0.1		
393	0.92	0.34	0.72	0.27
453	0.5	0.19	0.26	0.09
573	8.8×10^{-3}	3.3×10^{-3}		

[a] The absorbance, log (I_0/I), where I_0 and I are the intensities of incident and transmitted radiation. [b] The concentration of CO attached to Au^+ sites calculated using the Lambert−Beer law, $A = \epsilon cd$, where ϵ is the extinction coefficient (cm/μmol), c is the concentration (μmol/cm^2), and d is the path length (cm).

the XPS analysis that revealed the close proximity of Al cus sites to the charged Au species deep inside the zeolite lattice. With regard to these results, one undoubtedly can mention that the Al cus were responsible for activating the strong chemisorption of CO on Au^+ sites through the Al−O−Au linkage rather than the Al−Cl−Au one.

4. In Situ FT-IR of CO Adsorption on Au^{n+}/dM in the 2270−1800 cm^{-1} Region. Figure 4 shows the IR spectra of CO (50 Torr) adsorption at room temperature on the Au^+/dM sample, degassed at 343 K for 1 h, followed by evacuation of CO at increasing temperatures up to 473 K. Two principal spectral features were observed throughout the spectra: the band at 2192 cm^{-1} that was characterized by linearly bonded CO on Au^+ [12] and a broad band at 1949 cm^{-1} which was unexpected. However, this band was not observable for CO adsorption onto Au^+/NaY[12] and on Au^+/ZSM-5.[13]

The persistence of this band during thermal evacuation up to 473 K reflects that this band is neither artifact nor related to physisorbed species. A careful subtraction of the zeolite spectrum was performed for all the spectra in order to avoid the overlapping of the stretching Si−O overtone band in this region. In addition, adsorption of CO onto the bare zeolite showed no bands in that region. An interpretation for the 1949 cm^{-1} band could be perturbed CO_2 species as proposed by Busca and Lorenzelli.[29] However, this explanation is less probable in view of the limited stability of perturbed CO_2 species, which are quite labile upon evacuation.[29] Furthermore, one cannot assign the band to organic carbonates because activation at temperatures higher than 800 K is necessary for their desorption.[30] From the shape of band broadening and position as well as its thermal stability, one can propose that this band might be due to a strongly held bridging carbonyl-Au species. A similar result was obtained when CO adsorbed on CuY that resulted in uniform clusters (Cu−CO−Cu).[31]

With increasing the evacuation temperature, the surface coverage of the Au^+−CO species decreases whereas that of the bridging carbonyl species showed a comparatively less rapid decrease. This result is consistent with the theoretical calculations carried out by Santen,[32] that suggested that the ratio of bridging to linearly adsorbed CO increases with increasing the electron density of metal particles. The presence of residual water molecules inside zeolite throughout steaming helps in reducing Au species

(28) Knözinger, H. In *Elementary Reaction Steps in Heterogeneous Catalysis*; Joyner, R. W., Van Santen, R. A., Eds.; Kluwer Academic: Dordrecht, 1993; p 267.

(29) Busca, G.; Lorenzelli, V. *Mater. Chem.* **1982**, *7*, 89.

(30) Frieman, R. M.; Freeman, J. J.; Lytte, F. W. *J. Catal.* **1971**, *55*, 10.

(31) Davy Dov, A. A. *Infrared Spectroscopy of Adsorbed Species on the Surface of Transition Metal Oxides*; John Wiley and Sons: New York, 1990; p 85.

(32) Santen, R. V. *J. Chem. Soc., Faraday Trans. 1* **1987**, *83*, 1915.

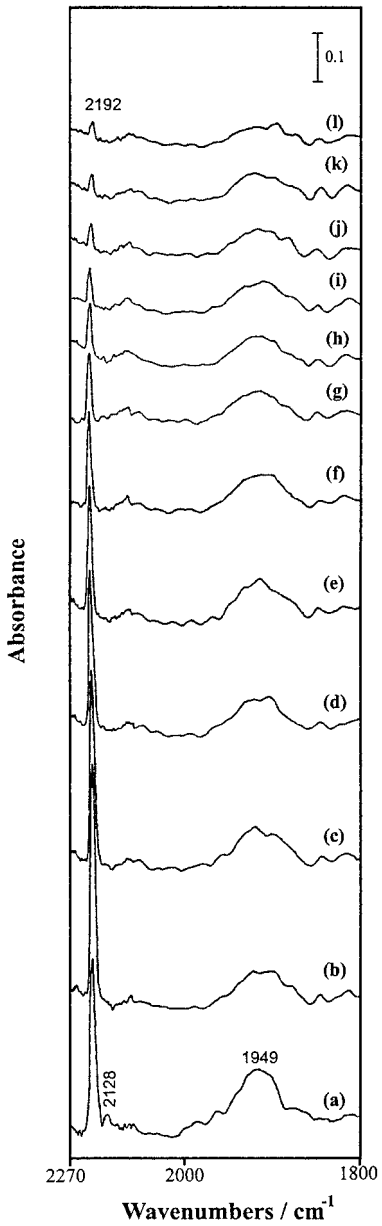

Figure 4. In situ FT-IR spectra of CO (50 Torr) adsorbed at room temperature on the treated Au^{n+}/dM sample at 343 K for 1 h. The system was evacuated while raising the temperature to (a) 343, (b) 363, (c) 373, (d) 383, (e) 393, (f and g) 403, (h) 413, (I) 423, (j) 433, (k) 443, and (l) 473 K.

to lower states, thereby increasing the electron density of the metal particles.[12] A similar result was also reported for Pt clusters entrapped inside NaY zeolite,[33] that showed the necessity of the copresence of water and CO to produce bridged as well as linear carbonyl species. From the foregoing results, the evolution and stability of the bridging CO is indeed associated with water−cation interaction inside the zeolite.

5. TPR Study of Au^{n+} Supported on dM, ndM, and NaY Zeolite Catalysts. An additional insight into the reducibility of charged Au species in the different samples was provided by the TPR profiles (Figure 5). No H_2 consumption peaks were observed for pure dealuminated H-mordenite zeolite. Meanwhile, the profiles of Au^{n+}/dM and Au^{n+}/ndM samples on one hand and that of Au^{n+}/NaY on the other hand showed noticeable differences. For

(33) Wang, R.-J.; Fujimoto, T.; Shido, T.; Ichikawa, M. *J. Chem. Soc., Chem. Commun.* **1992**, 962.

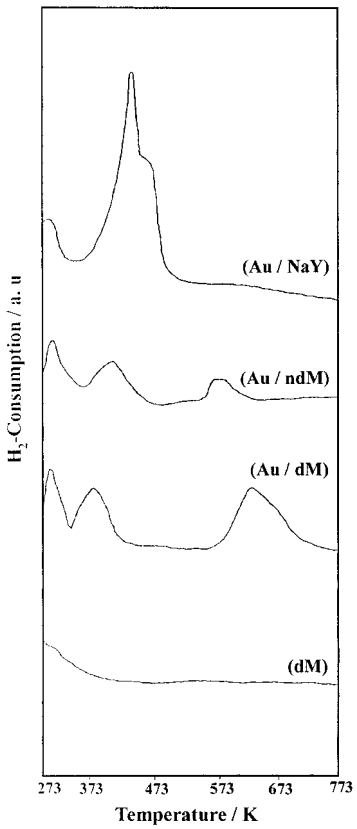

Figure 5. TPR profiles of dealuminated H-mordenite (dM), Au^{n+}/dM, Au^{n+}/ndM, and Au^{n+}/NaY zeolite catalysts.

all Au^{n+}/zeolite samples, the first temperature peak at 293 K in the TPR patterns is associated with the reduction of some of Au(III) into Au(I) species. This was consistent with the result of Salama et al.,[12] who confirmed the reduction of some Au cations during hand grinding of the $AuCl_3$−zeolite mixture at room temperature. The complete reduction of Au(III) into Au(I) is accomplished by the development of a second peak in the 373−413 K range. From a TPD study of physically mixed $AuCl_3$ with partially dehydrated NaY, HCl (m/e = 36) was evolved in this temperature range. Consequently, the high-temperature peak represents the reduction of Au(I) into Au(0). This peak showed maxima at 633, 573, and 433 K in the profiles of Au^{n+}/dM, Au^{n+}/ndM, and Au^{n+}/NaY, respectively. The earlier appearance of the third reduction peak of Au^{n+}/NaY compared with those of Au^{n+}/dM and Au^{n+}/ndM could be due to the lower dispersion of Au^{n+} species in the former sample than in the latter samples. The temperature discrepancies in reduction profiles of the three samples can be explained by either morphological changes in Au^{n+} crystallites and/or from variation of Au^{n+}−zeolite interactions. From the above-mentioned observations, one may state that Au^{+} species encapsulated inside dM zeolite are more stable compared with those inside ndM and NaY.

The amount of consumed H_2, calculated from the area under the two peaks in the 373−633 K region, divided by the initial amount of Au in μmol g^{-1} catalyst (H_2/Au), indicates ratios of 1.19, 0.33, and 0.94 for Au^{n+}/dM, Au^{n+}/ndM, and Au^{n+}/NaY, respectively. The higher ratio provided by Au^{n+}/dM gives us a clue that Au^{n+} was present in a higher amount than in the other samples.

Conclusions

1. The creation of coordinatively unsaturated Al species inside the mordenite zeolite by steaming enhanced the

adsorption of Au(I) toward CO giving rise to a characteristic band at 2192 cm^{-1}. This band showed a remarkable thermal stability up to 521 K. An interaction of Al with the zeolitic lattice oxygen and Au^{n+} species was proposed on the basis of the results presented by XRD and XPS analyses.

2. The water contained inside the zeolite upon steaming is conceivably responsible for the evolution of the bridged bonded CO that showed a considerable stability even at an evacuation temperature as high as 473 K. Indeed, the revelation of stable bridged carbonyls on Au^{n+}/dM was reported for the first time under the present conditions.

3. The TPR results showed that Au^{n+} species in dM zeolite are relatively more resistant to reduction than those in ndM and NaY zeolites. These results are in agreement with those obtained from the IR and XPS data.

LA001403F